Reactive Sintering of TiAl-Ti_5Si_3 Insitu Composites

David E. Alman
U.S. Department of Energy - Albany Research Center
Albany, OR 97321-2198, USA
(541) 967-5885; Fax: (541) 967-5845: Email:alman@alrc.doe.gov

Abstract

TiAl with between 0 and 20 volume percent (v%)Ti_5Si_3 was produced by reactive sintering of cold pressed compacts of elemental Ti, Al and Si powder mixtures at 700°C for 15 minutes in vacuum. The results show that adding Si to Ti and Al reduces the swelling associated with reactive sintering of TiAl, as composites containing more than 5 v%Ti_5Si_3 densified during reactive sintering. However, composites containing more than 10v% Ti_5Si_3 did not retain their shape during processing, and the TiAl+20v% Ti_5Si_3 composite completely melted during the sintering process. A thermodynamic analysis indicated that the simultaneous formation of TiAl and Ti_5Si_3 increases the adiabatic flame temperature during the reaction between the powders. In fact, the analysis predicted that the maximum temperature of the reaction associated with the formation TiAl+20v% Ti_5Si_3 should exceed the melting point of TiAl, and this was observed experimentally. Differential thermal analysis (DTA) revealed that a Al-Si eutectic reaction occurred in mixtures of Ti, Al and Si powders prior to the formation of the TiAl and Ti_5Si_3 phases. There was no such pre-reaction formation of an eutectic liquid in Ti and Al powder mixtures. The formation of the pre-reaction liquid and the increase in adiabatic flame temperature resulted in the melting that occurred and the enhanced densification (minimization of swelling) during reactive sintering of the insitu composites.

Key words: reactive sintering, TiAl, Ti_5Si_3, insitu composites, Self-propagating High-temperature Synthesis (SHS).

Introduction

Reactive sintering involves forming compounds or composites from elemental or sub-compound constituents, typically in powder form. During processing, a Self-propagating, High-temperature Synthesis (SHS) reaction (also termed combustion synthesis) occurs within an intimate powder mixture, transforming the powders into the desired compound. The driving force for the reaction is the negative heat of mixing of the resultant compound. The chemical reaction results in a release of energy (heat), that sustains and propagates the reaction throughout the body of the reactants. Typically, these reactions initiate at a low homologous temperature. For aluminide compounds, the reactions initiate near or at the melting point of Al (660°C). In many cases, the reaction is accompanied by the formation of a transient liquid phase; and as with any liquid phase sintering operation, densification occurs due to capillary effects associated with liquid formation. The prototype example of this process is the reactive sintering of Ni_3Al, where near fully dense (i.e., >99%) Ni_3Al articles were produced by sintering a stoichiometric mixture of Ni and Al powders at 750°C (T_H=0.6) for 15 minutes in vacuum [1,2]. Densification coincided with the initiation of the reaction in the powder mixture and factors that alter the amount, distribution, and duration (i.e, powder particle size, green density, heating rate, sintering atmosphere, etc.,) of the transient liquid phase affected the density of the final Ni_3Al product [1,2].

The product that forms upon reactive sintering a mixture of Ti and Al powders with a composition corresponding to the intermetallic compound TiAl is quite porous. In fact, the density decreases upon sintering and the physical dimensions of the powder compact increase (i.e., the specimen swells). The generation of porosity has been attributed to several factors, and include [3-10]:

(i) *Kirkendall porosity* due to unbalanced diffusivities. Al diffuses faster in Ti, than does Ti in Al. The result is a pore in the product where the Al powder resided prior to the initiation of the reaction.

(ii) *Gas evolution* due to the volatization of impurities at the powder surfaces. Commercial Ti powders tend to have a high residual impurity (particularly chloride) content [11], and the heat generated by the reaction is sufficient to volatize these impurities, which may prevent densification.

(iii) *Molar volume effects* due to differences in the intrinsic densities of the product and the reactants. TiAl is more dense than the corresponding mixture of Ti and Al powders by about 5.2% [7]. Porosity will be generated in the product unless the dimensional change (shrinkage) of the product during sintering equals or exceeds this volume decrease [7].

In any event, to produce dense TiAl from a mixture of elemental Ti and Al powders, pressure must be applied, in some form, during reactive processing [12-22].

This investigation examines the influence of Si additions on the microstructure of the product that forms during the reactive sintering of Ti and Al powder mixtures. This was undertaken, based on the results of a previous study [12,13], which found that reactive hot-pressed TiAl-Ti_5Si_3 insitu composites could be processed to higher density (less porosity) than comparable monolithic TiAl or Ti_5Si_3 under similar processing conditions.

Experimental Procedure

Commercially available powders were utilized for this study. The Ti powders were produced via the hydride-dehydride process, were irregularly shaped and classified as –325 mesh

(45μm) in size. The Al powders were produced by helium atomization and were spherical in shape with an average diameter of 15μm. The Si powders were produced by milling. The morphology of these powders was angular and classified as –325 mesh (45μm) in size. Elemental powder blends corresponding to TiAl with 0, 5, 7.5, 10, 12.5 15, and 20 volume percent (v%) Ti_5Si_3 were prepared by mixing the powders in glass jars using a Turbula-type mill. Green compacts were produced by cold pressing approximately 5 grams of blended powders in a 12.5 mm in diameter cylindrical steel die. To prevent any contamination of the Ti powders, no die lubrication was used during compaction. The green densities were determined by dividing the weight of the compacted cylinder by its apparent volume. The green compacts were sintered in vacuum a furnace equipped with an ordinary diffusion pump. The samples were heated at a rate of 10°C/min to 700°C and held at 700°C for 15 minutes, after which they were furnace cooled. The sintered densities were determined via the Archimedes (water immersion) method or by dividing the sintered weight by volume (from dimensions). The microstructures of the resultant specimens were analyzed using optical and scanning electron microscopy.

Results

Table I lists relevant dimension of the compacts before and after reactive sintering. Figure 1 shows macro-photographs and Figures 2 through 6 show optical microstructures of the compacts after reactive sintering. As expected, the physical dimensions of the monolithic TiAl increased (swelled) with a concomitant increase in porosity and a decrease in density. The microstructure of TiAl was sponge-like, with interconnected porosity (Figure 2). This microstructure is typical for reactively sintered TiAl.

Similar to monolithic TiAl, the reactive sintered TiAl+5v%Ti_5Si_3 compact consisted of interconnected porosity (Figure 3). However, unlike monolithic TiAl, the distribution of the porosity was non-uniform in the TiAl+5v%Ti_5Si_3. A dense rim formed at the outer edge on the top portion of the specimen, where as at the bottom of the specimen the structure was very porous.

Composites with 7.5v% and 10v% Ti_5Si_3 densified during reactive sintering (Table I). The "hour-glass" shape of these compacts was probably due to density gradients that developed in the compact during die pressing, a consequence of not utilizing die lubrication. (Density gradients in pressed powder compacts can translate into anisostropic shrinkage during sintering, resulting in an "hour-glass" shape [23].) The microstructure of these composites consisted isolated pores surrounded by relatively dense matter in the center of the compacts with the outer rim of the compacts nearly pore free (Figures 4 and 5).

Composites with greater than 10v% Ti_5Si_3 did not retain their shape during reactive sintering (Figure 1). The TiAl+12.5 and 15v% Ti_5Si_3 composites appeared to slump, while the TiAl+20v% Ti_5Si_3 sample completely melted (Figure 1). In the proximity of the shape distortion, the microstructure of the 12.5 and 15v% Ti_5Si_3 composites consisted of extremely large pores (Figure 6), and were most probably due to entrapped gas. These pores were surrounded by relatively dense material, and like the 7.5 and 10v% Ti_5Si_3 composites, the outer rim was nearly pore free (Figure 6).

Illustrated in Figure 7 are backscattered SEM images of the monolithic TiAl, and the TiAl+7.5v%Ti_5Si_3 andTiAl+15v%Ti5Si_3 composites. The microstructure of the TiAl specimen contains un-reacted Ti particles surrounded by a Ti_3Al reaction zone. The TiAl+7.5v%Ti_5Si_3 composite contains needle-like Ti_5Si_3 particles within the TiAl matrix. The matrix also contains

un-reacted Ti surrounded by a Ti_3Al reaction zone. The 15v% Ti_5Si_3 composite is comprised of a "necklace" of needle-like Ti_5Si_3 particles within the matrix. There are considerably fewer un-reacted Ti particles in the microstructure, as evidenced by the more uniform contrast of the TiAl matrix in the backscattered images.

Discussion

The results showed that adding Si to a Ti and Al mixture reduces the swelling associated with the reactive sintering of TiAl. The pore structure changed from one consisting of interconnected porosity (monolithic TiAl) to one consisting of isolated pores in the composite mixtures. The rationale for this behavior is discussed below.

Differential Thermal Analysis (DTA) was used to characterize the reactions within the powder mixtures. DTA data was collected on a Netzsch 409 DTA . All DTA runs were performed under flowing ultra high purity Ar (100 ml/min). The specimens (20 to 40 mg of mixed powders, hand pressed into Al_2O_3 crucibles) were heated from room temperature to either 800 or 1000°C at a rate of 10°C/min. Scans performed on an elemental powder mixtures corresponding to monolithic Ti_5Si_3, were also done. The DTA scans are shown in Figure 8 and these traces are similar to those reported by Roa and Du [20] for mechanically alloyed Ti, Al and Si powders.

The DTA trace for the binary Ti and Al powder mixture showed an exothermic reaction at 660°C (arrow A on Figure 8). This corresponds to transformation of the elemental powders to the TiAl. For mixtures containing Ti, Al and Si powders, an endothermic reaction occurred at 580°C (arrow B on Figure 8) prior to two exothermic reaction (arrows C and B on Figure 8). The

endothermic reaction corresponded to eutectic reaction melting of the Al and Si, while the exothermic reactions are associated with the formation of TiAl and Ti_5Si_3.

The difference between reactions that occur in the binary Ti-Al and ternary Ti-Al-Si mixture is the formation of the eutectic liquid in ternary mixture. As with traditional liquid phase sintering, the capillary forces associated with the formation of the eutectic cause the dimensions of the compact to shrink resulting in densification. Further, it is feasible that the formation of the Al-Si liquid acts as a high diffusivity path, which minimizes the formation of Kirkendall porosity in composites produced from Ti, Al and Si powder mixtures.

The melting observed in the high volume fraction Ti_5Si_3 composites can be attributed to the adiabatic flame temperature (i.e., maximum temperature) of the reactions. The theoretical adiabatic flame temperature (T_{ab}) can be determined from a simple energy balance as follows [24]:

$$\Delta H_f^{T_o} = \int_{T_o}^{T_{ab}} C_p dT$$

where (T_O) is a reference temperature, usually 298K. ($\Delta H_f^{T_o}$) is the enthalpy of formation of the product at the reference temperature and (C_p) is the specific heat of the product. If a portion of the product melts, the energy balance is modified accordingly:

$$\Delta H_f^{T_o} = \int_{T_o}^{T_{ab}} C_p dT + v\Delta H_m$$

to account for the heat of fusion (ΔH_m) of the product and the fraction *(v)* of product in the molten state., HSC Chemistry for Windows* chemical reaction and equilibrium software and thermochemical data base was used to calculate the adiabatic flame temperature for the following reaction:

$$(x + 5y)Ti + xAl + 3ySi \rightarrow xTiAl + yTi_5Si_3$$

The results are and shown in Figure 9 as a function of Ti_5Si_3 content in TiAl. The adiabatic flame temperature of the reactions to form TiAl with greater than 5 atomic percent (which corresponds to approximately 20 vol%, Ti_5Si_3) exceeds the melting point of TiAl, which is what was observed experimentally.

---

*Reference to specific products or vendors does not imply endorsement by the U.S. Department of Energy

Based on the backscattered microstructures in Figure 7, as the amount of Ti_5Si_3 increases in the composites, the microstructure of the TiAl phase becomes more uniform with less un-reacted Ti-particles remaining after reactive sintering. It should be pointed out that similar results were observed in hot-pressed composites. The TiAl matrix of TiAl+Ti_5Si_3 composite was more homogenous than monolithic TiAl hot-pressed under identical conditions [12,13]. As the above analysis has shown, the adiabatic flame temperature increases with increasing Ti_5Si_3 content. This increase in temperature facilitates faster and more complete diffusion of the reactants resulting during reactive sintering, leading to more homogenous microstructures.

The microstructure of the TiAl+Ti_5Si_3 composites consists of pores in the center of the compact with a nearly pore–free outer rim. This microstructure indicates that the pores in the center of the compact form as a result of trapped volatized gases. This occurred because the specimens were processed by heating the compacts in tube furnace. Thus, the surfaces of the compacts were essentially uniformly heated and SHS-type reaction initiated in the "explosion mode". That is, the reaction initiated from multiple surface sites and propagated inwards towards the sample center. As the surface of the specimen densified gases generated in the interior of the

specimen had no pathway of escape, resulting in the formation of pores. As a result, the Archimedes densities listed on Table I are not accurate, as the entrapped gas results in higher density values during measurement. It is feasible that the porosity may be eliminated in the composites if the reaction is controlled via initiation of the reaction in the "propagation mode". That is, utilizing a point source to heat a specific location on the surface. The reaction will then propagate through the powder compact from this point in a more controlled manner. This will allow for gas generated in the interior to escape through the porous compact ahead of the reaction front.

Conclusion

This study has shown that the addition of Si to mixtures of Ti and Al powders is beneficial to densification during reactive sintering of TiAl. The simultaneous formation of TiAl and Ti_5Si_3 tends to eliminate the Kirkendall porosity that is usually seen during reactive sintering monolithic TiAl. The rationale for this behavior is attributed to the formation of a pre-reaction Al-Si eutectic and an increase in the adiabatic flame temperature during reactive sintering of TiAl-Ti_5Si_3 insitu composites as compared to the reactive sintering of monolithic TiAl.

Acknowledgements

The author would like to acknowledge R.D. Govier, W.K. Collins, D.L. Davis, A. Hunt and P. Danielson, all of the Albany Research Center, for assistance with performing the experiments. The author would also acknowledge the helpful discussions with my colleagues at the Albany Research Center, Dr. J. A. Hawk, Dr. C.P. Dogan and Mr. A.V. Petty, Jr.

References

1. A. Bose, B. Moore, R.M. German, and N.S. Stoloff, *J. Met.*, **40 (9)**, 1988, 14.
2. D. Sims, A. Bose, and R.M. German, *Prog. Powder. Met.* **43**, 1987, 575.
3. A.P. Savitskii, *Liquid Phase Sintering of Systems with Interacting Components*, Russian Acadamy of Sciences, Tomsk, 1993.
4. G.X. Wang and M. Dahms *Powder Metall. Int.*, **24 (4)** 1992, 212
5. M. Dahms and F. Schmelzer, *Z. Metallk.*, **84 (5)** 1993, 351.
6. K. Shibue, Sumitomo *Light Met. Tech. Rep.* **32**, 1992, 351.
7. R.W. Rice and W.J. McDounough, *J. Am. Ceram. Soc.* **68**,1985, C122.
8. A. Bohm, T. Jungling and B. Kieback, in *Advances in Powder Metalluragy and Particulate Materials –1996, Part 10,* eds. T.M. Cadle and K.S Narasimhan, MPIF, Princeton, NJ, 1996, p. 51.
9. D.C. Dunand, *Mater Manuf. Process.*, **10, (3)** 1995, p. 373.
10. R.R. Oddone and R.M. German, in *Advances in Powder Metalluragy and Particulate Materials –1989, vol.3* , eds T.G. Gasbarre and W.F. Jandeska, MPIF, Princeton, NJ, 1989, p. 475.
11. S.J. Gerdemann and D.E. Alman, "in *Advances in Powder Metalluragy and Particulate Materials –2000, Part 12* , eds. H. Ferguson and D.T. Whtchell, Sr., MPIF, Princeton, NJ, 2000, p. 41.
12. D.E. Alman, J.A. Hawk, and M. Ziomek-Moroz, *in Insitu Reactions for the Synthesis of Composites, Ceramics and Intermetallics*, eds., E.V. Barrera, S.G. Fishman, F.D.S. Marquis, N.N. Thadhani, W.E. Frazier, and Z.A. Munir, TMS, Warrendale, PA, 1996, p. 41.
13. D.E. Alman, J.A. Hawk and C.P. Doğan, in *Advances in Powder Metalluragy and Particulate Materials –1995, Part 7* , eds. M. Phillips and J. Porter, Sr., MPIF, Princeton, NJ, 1995, p.175.
14. J.C. Rawers and W.R. Wrzesinski, *J. Mater. Sci*, **27**, 1992, 2877.
15. G-X. Wang and M. Dahms, *JOM* ,**45 (5)**, 1993, 52.
16. G-X. Wang and M. Dahms, *Metall. Trans. A*, **24A**, 1993, p. 1517.
17. C.E. Wen, K. Yasue, and Y. Yamada, *J. Mater. Sci*, **36**, 2001, 1741.
18. J.B. Wang and W.S. Hwang, *J. Mater. Engr. Perf.* **7 (3)**, 1998, 385.
19. K. Taguchi, M. Ayada, K.N. Ishihara and P.H. Shingu, *Intermetallics*, **3**, 1995, 91.
20. K.P. Rao and Y.J. Du, *Mater. Sci,. Engr.*, **A277**, 2000, 46.
21. G-X. Wang, B. Dogan, F-Y. Hsu, H-J. Klarr and M. Dahms, *Metall. Mater. Trans,*, **26A**, 1995, 691.
22. O.N. Senkov, M. Cavusoglu and F.H. Froes, *Mater. Sci. Engr.*, **A300**, 2001, 85.
23. R.M. German, Powder Metallurgy Science, 2nd ed. MPIF, Princeton, NJ, 1994, p. 267.
24. N.A. Gokcen: Thermodynamics, Techscience Incorporated, Hawthorne, CA, 1975, p. 87.
25. A. Roine: HSC Chemistry for Windows, version 2.0, Outokumpu Research Oy. Fin. 28101 Pori, Finland, May 31, 1994

TABLE I
DIMENSION OF REACIVE SINTERED COMPACTS

Composite	Theoretical Density (g/cm^3)	Diameter (mm)		Shrinkage $(D_o-D_s)/D_o$ (%)	Green Density		Sintered Density	
		Green (D_o)	Sintered* (D_s)		(g/cm^3)	(% Theor.)	(g/cm^3)	(% Theor.)
TiAl	3.80	12.7	17.6	-38.4	3.05	80	1.37**	36
TiAl+5v%Ti_5Si_3	3.83	12.7	12.6	0.8	3.06	79	3.04**	79
TiAl+7.5v%Ti_5Si_3	3.84	12.7	11.7	7.9	3.06	79	3.73	97
TiAl+10v%Ti_5Si_3	3.85	12.7	12.0	5.5	3.06	79	3.62	94
TiAl+12.5v%Ti_5Si_3	3.86	12.7	12.3	3.2	2.99	77	3.32	85
TiAl+15v%Ti_5Si_3	3.88	12.7	12.3	3.2	2.98	76	3.37	86
TiAl+20v%Ti_5Si_3	3.90	12.7	n/m	n/m	3.01	77	n/m	n/m

n/m = not measured
***Sintered diameter measured from center of height; for 12.5 and 15v%Ti_5Si_3 specimens measured on cylindrical portion of compact, above melted region (see figure 1)**
****** Density measured by dividing weight by volume from dimensions, all others densities measured by the Archimedes (water immersion) method.**

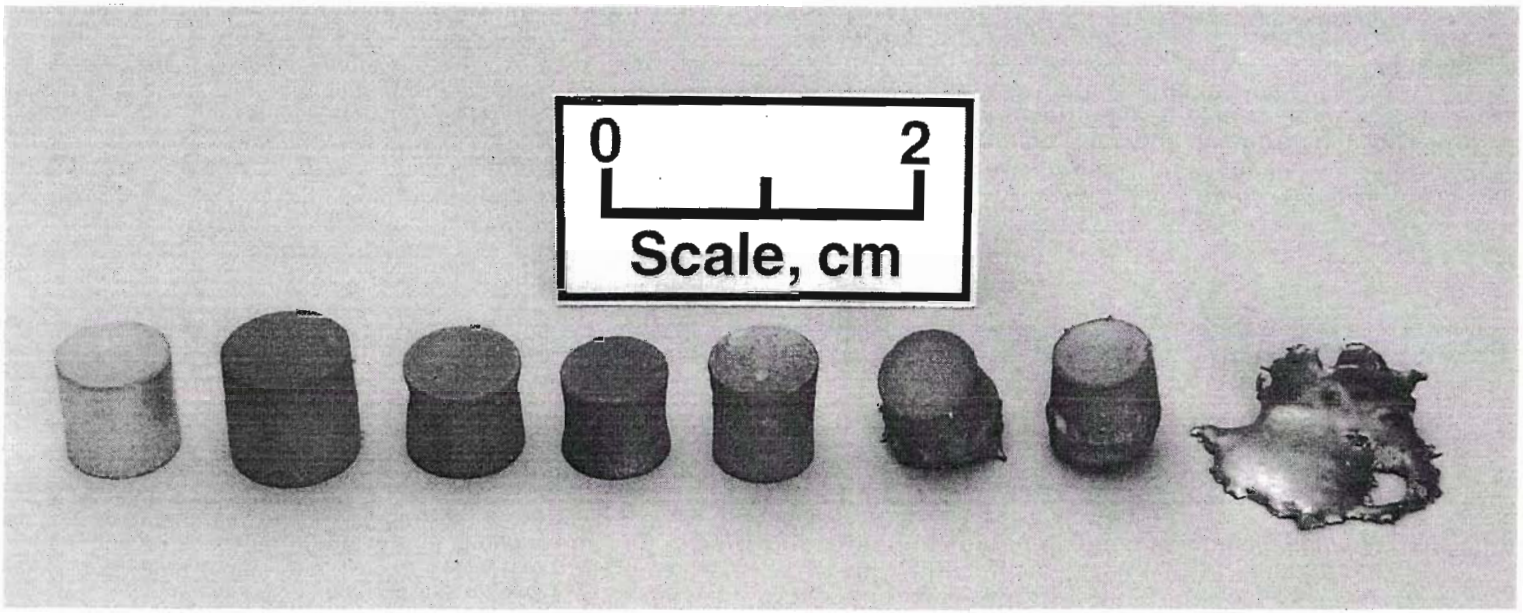

Figure 1. Macrophotograph of $TiAl+Ti_5Si_3$ composites produced by reactive sintering mixtures of Ti, Al and Si powders at 700°C for 15 minutes in vacuum (left to right: typical green compact; monolithic TiAl; $TiAl+5v\%Ti_5Si_3$; $TiAl+7.5v\%Ti_5Si_3$; $TiAl+10v\%Ti_5Si_3$; $TiAl+12.5v\%Ti_5Si_3$; $TiAl+15v\%Ti_5Si_3$; $TiAl+20v\%Ti_5Si_3$).

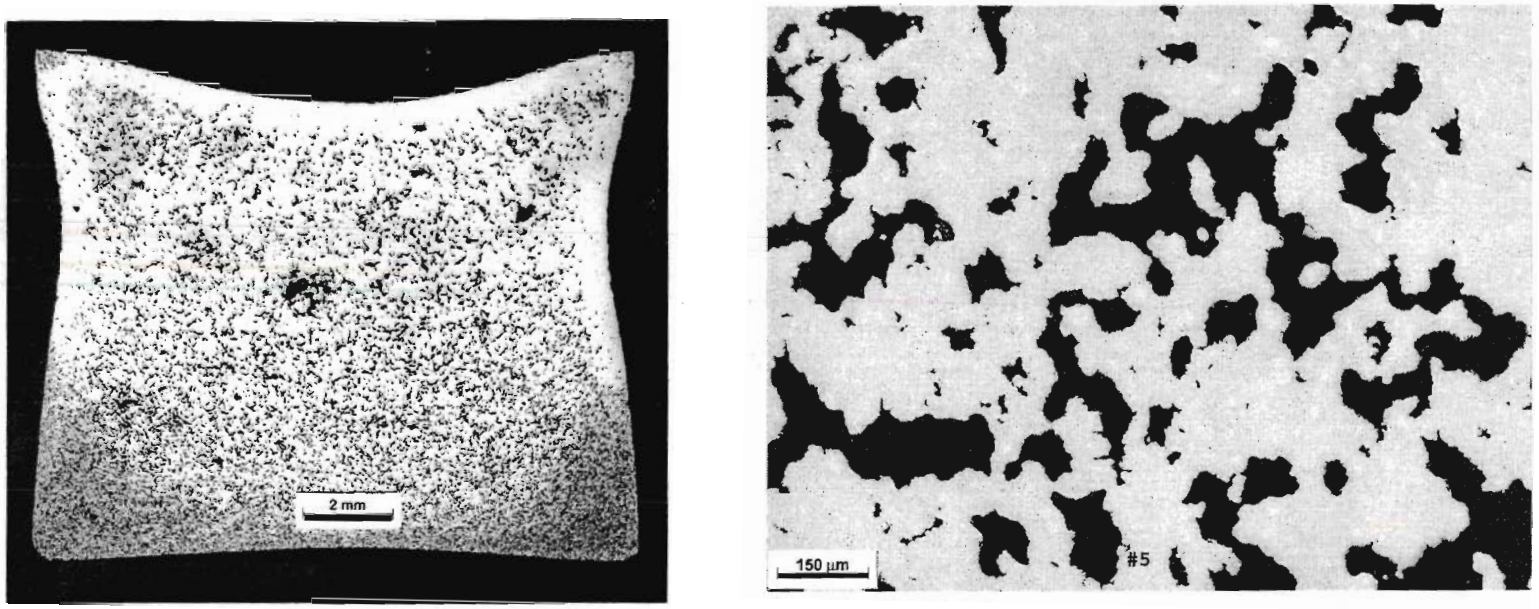

(a) (b)

Figure 3. Optical microstructure of reactive sintered TiAl+5v%Ti_5Si_3: (a) low magnification view showing entire specimen; (b) high magnification view from center of specimen. Black phase is porosity.

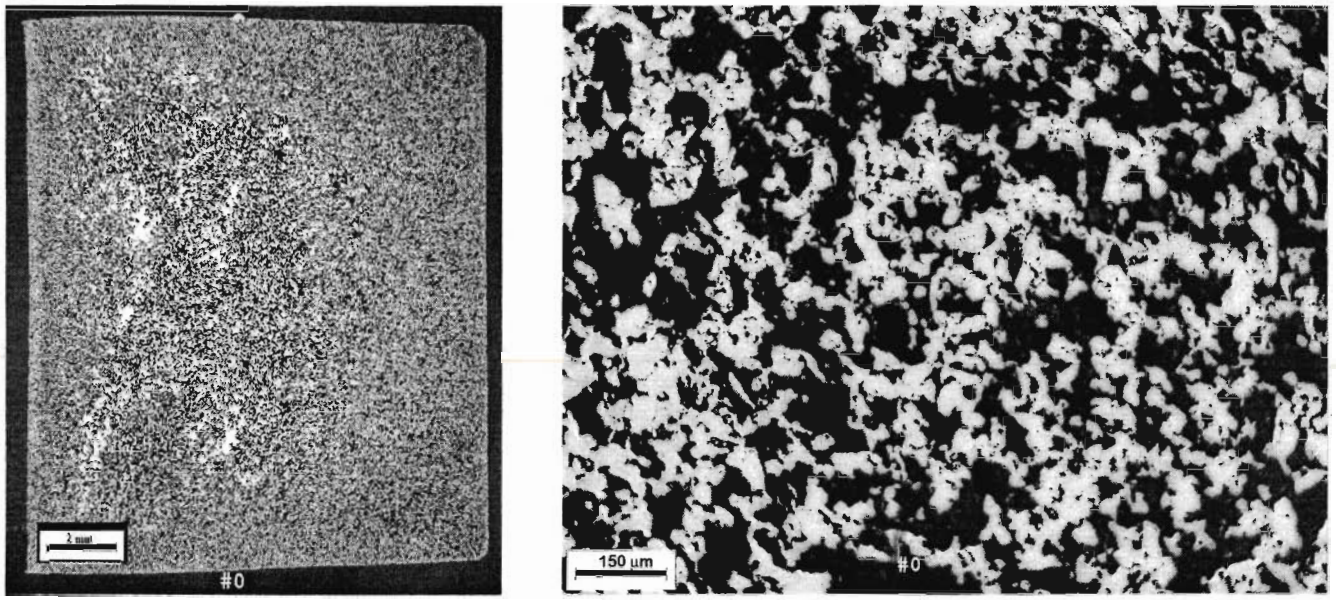

(a) (b)

Figure 2. Optical microstructure of reactive sintered TiAl: (a) low magnification view showing entire specimen; (b) high magnification view from center of specimen. Black phase is interconnect porosity in specimen.

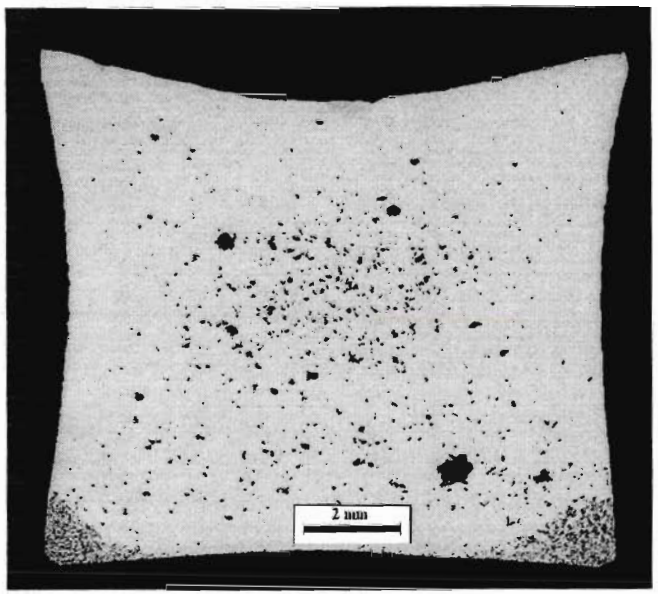

(a)

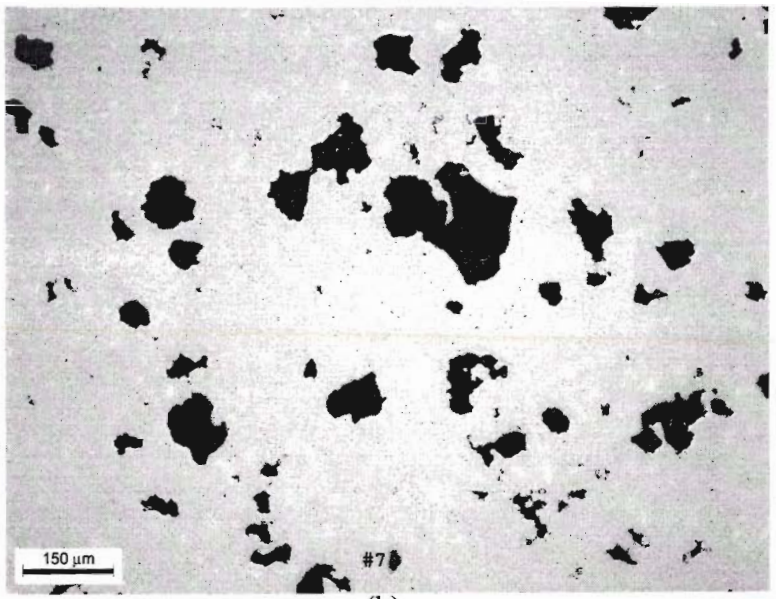

(b)

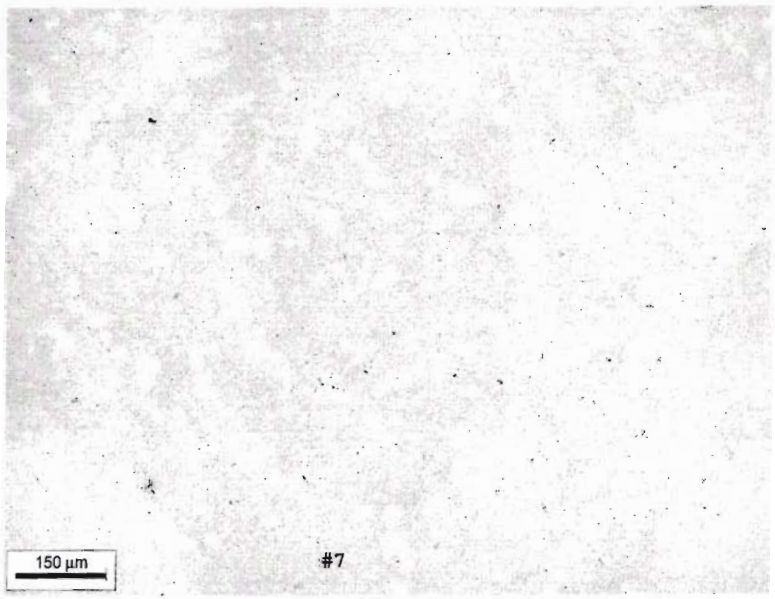

(c)

Figure 4. Optical microstructure of reactive sintered TiAl+7.5v%Ti_5Si_3: (a) low magnification view showing entire specimen; (b) high magnification view from center of specimen; (c) high magnification view from edge of specimen. Black phase is porosity.

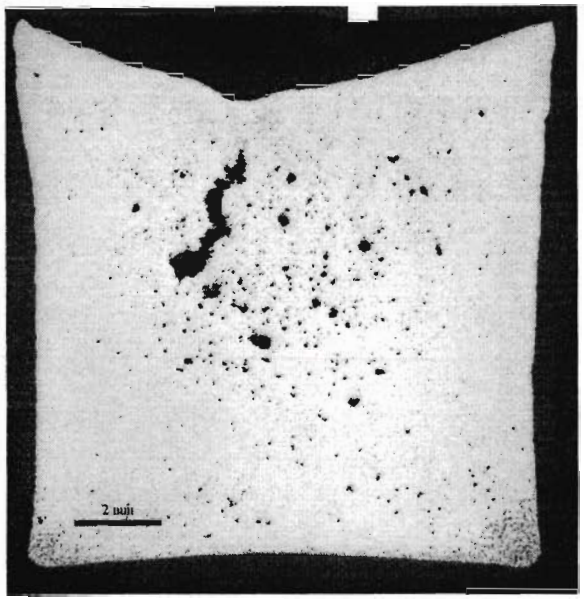

(a)

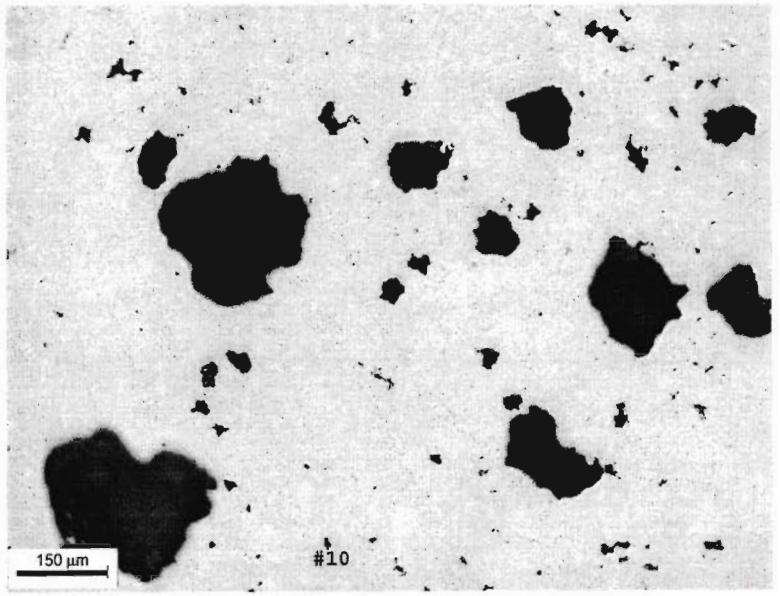

(b)

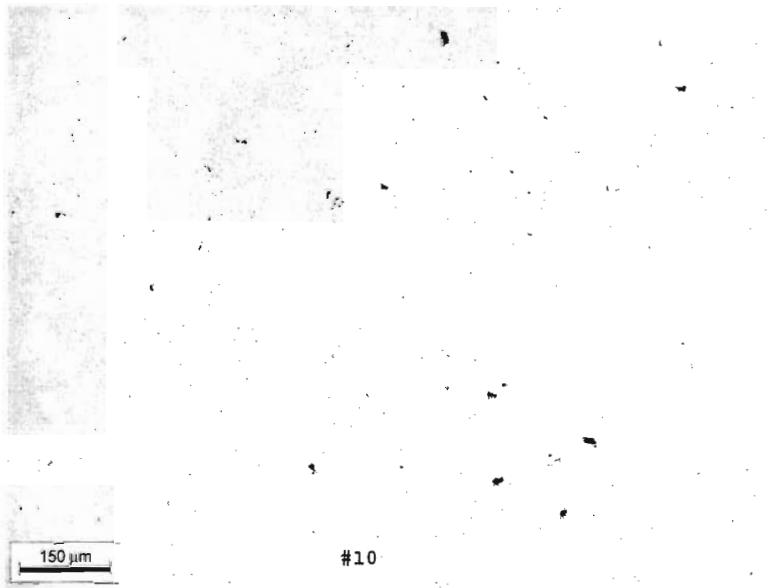

(c)

Figure 5. Optical microstructure of reactive sintered TiAl+10%Ti_5Si_3: (a) low magnification view showing entire specimen; (b) high magnification view from center of specimen; (c) high magnification view from edge of specimen. Black phase is porosity.

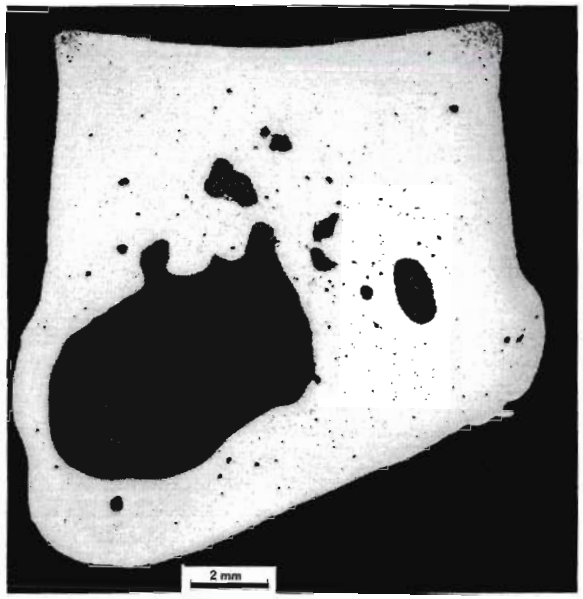

(a)

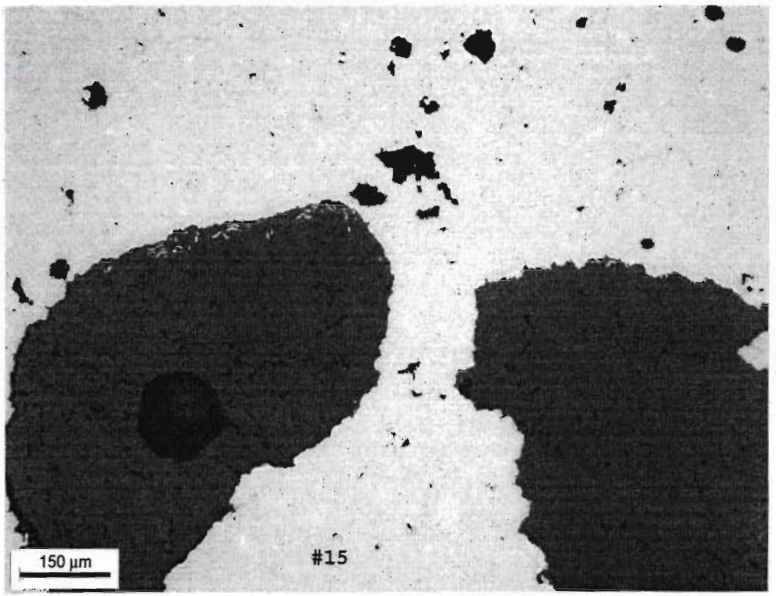

(b)

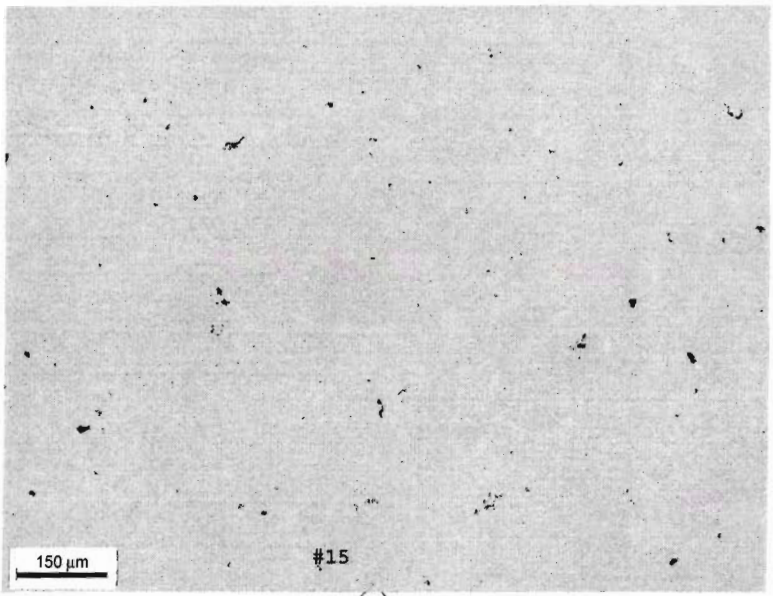

(c)

Figure 6. Optical microstructure of reactive sintered TiAl+15%Ti_5Si_3: (a) low magnification view showing entire specimen; (b) high magnification view from center of specimen;
(c) high magnification view from edge of specimen.

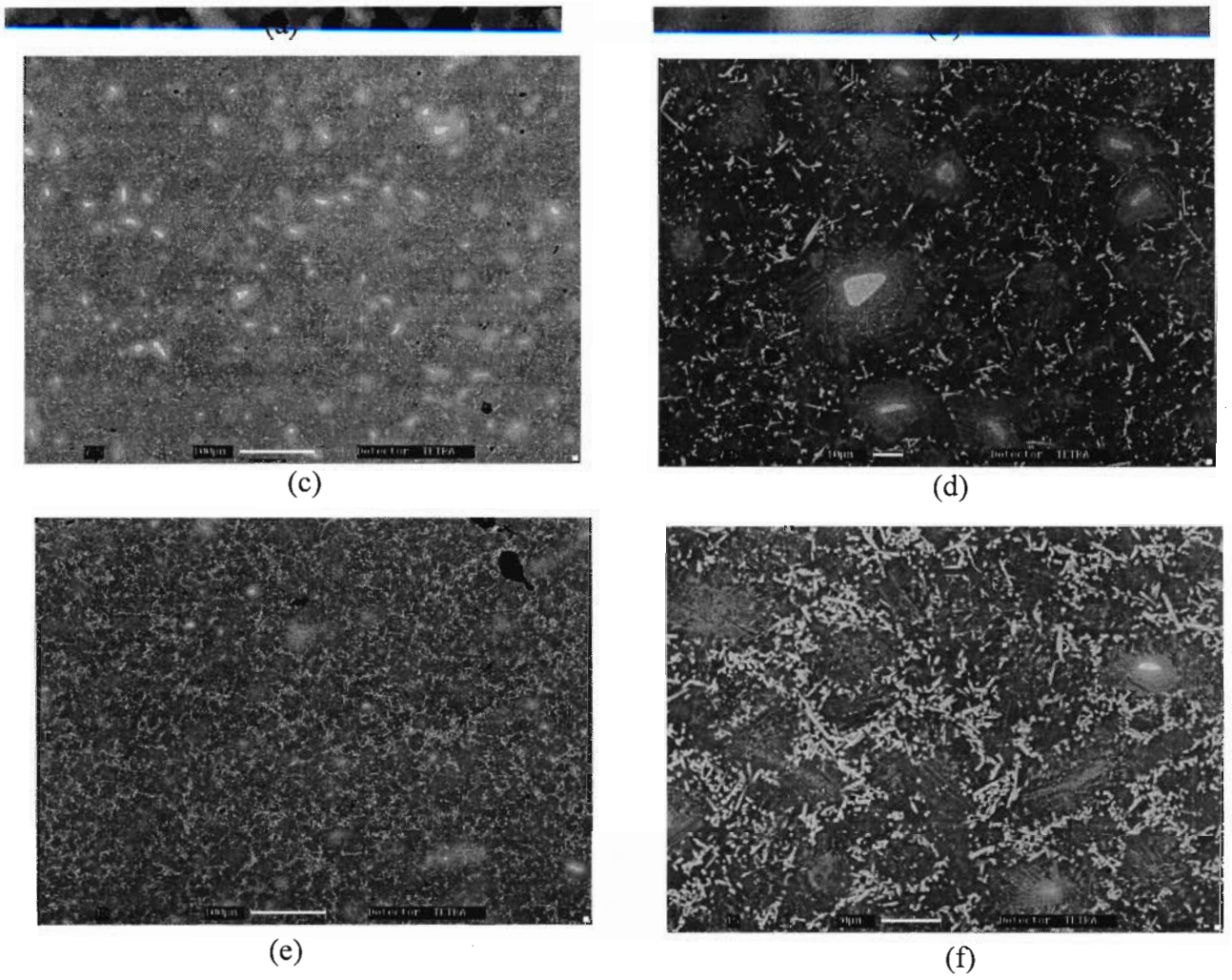

Figure 7. Backscattered electron micrographs of: (a) and (b) monolithic TiAl; (c) and (d) TiAl+7.5v%Ti_5Si_3 composite; and (e) and (f) TiAl+15v%Ti_5Si_3 composite.

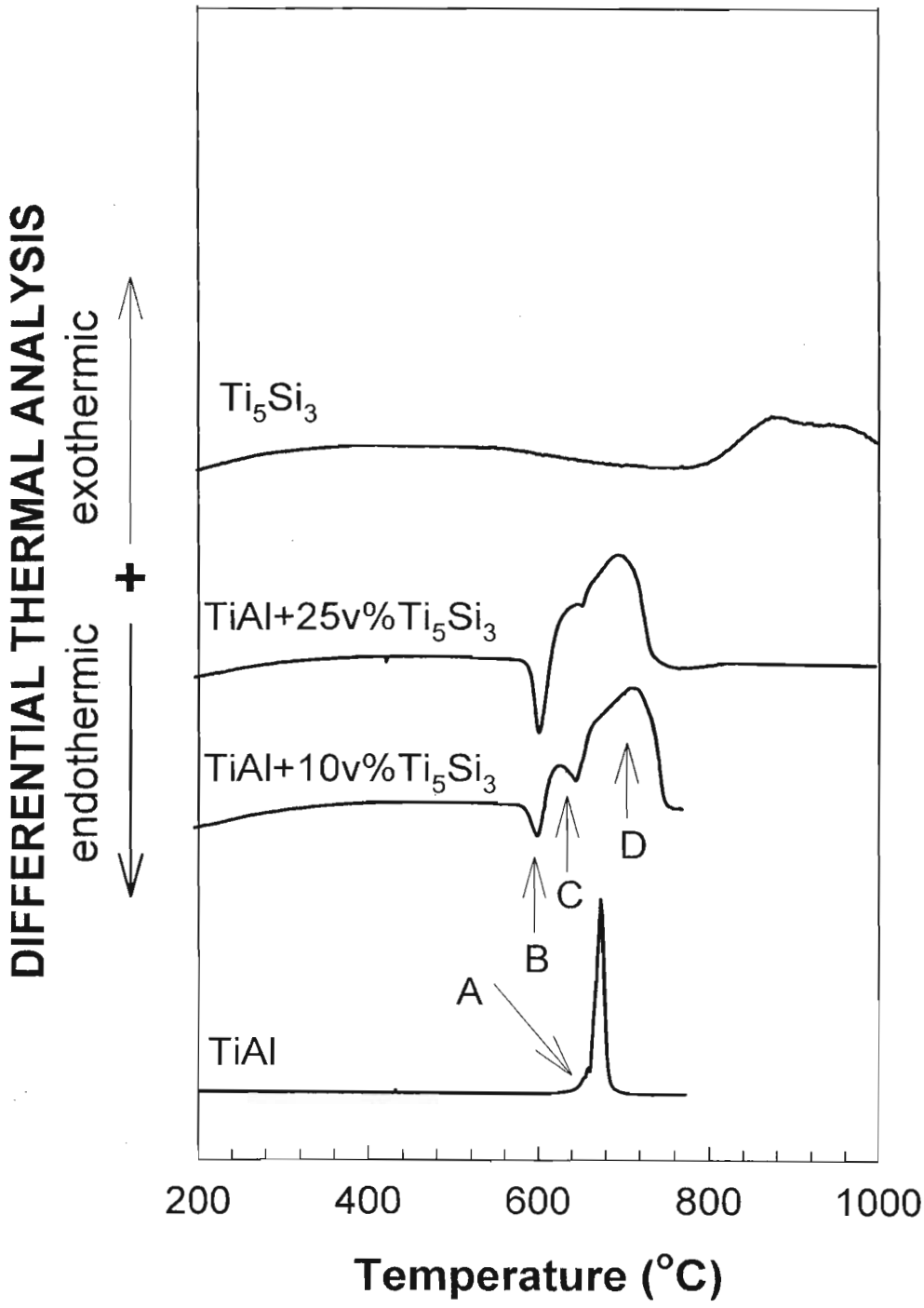

Figure 8. DTA traces obtained upon heating elemental Ti, Al and Si powder mixtures corresponding to TiAl, TiAl+10v% Ti_5Si_3, TiAl+25v% Ti_5Si_3 and Ti_5Si_3.

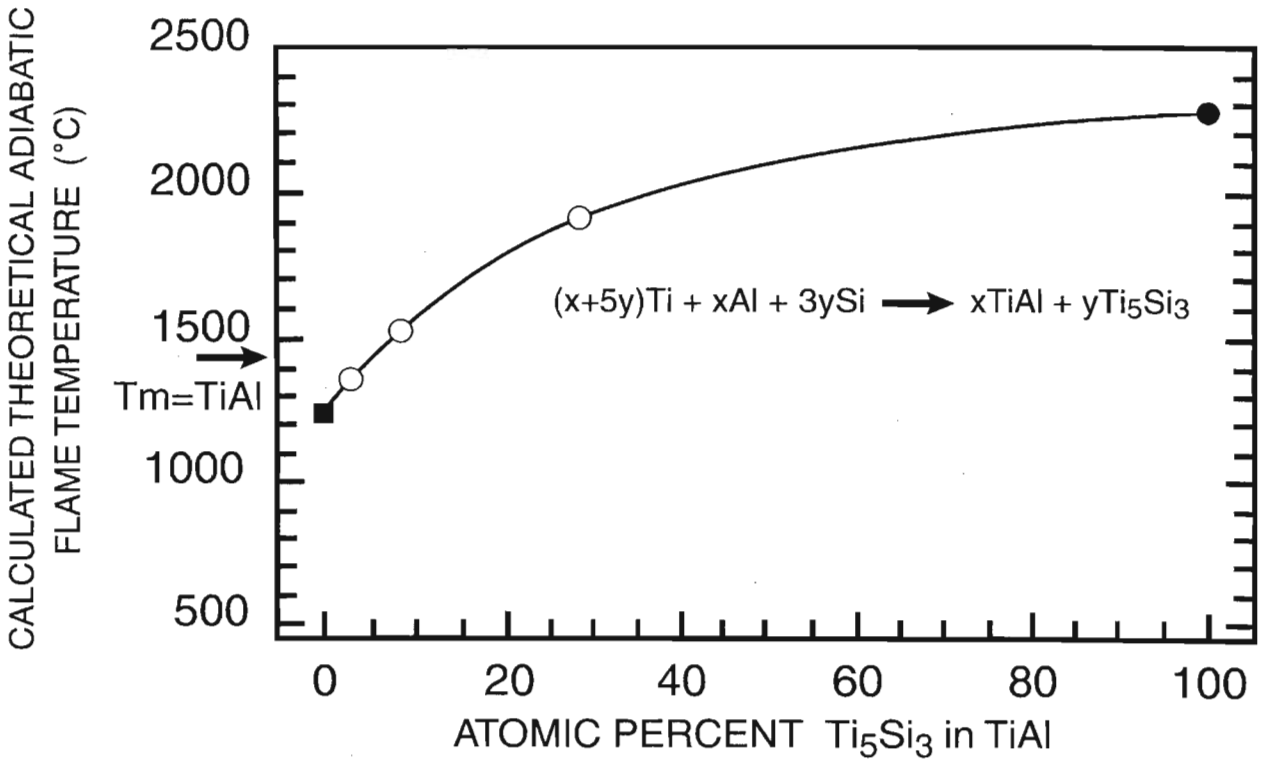

Figure 9. Calaculated adiabatic flame temperatures for the reaction to form TiAl+Ti_5Si_3 insitu composites from elemental constituents, as a function of Ti_5Si_3 content.